JOURNAL OF CATALYSIS 143, 92–101 (1993)

The Kinetics of Propylene Metathesis Catalyzed by a Molybdenum (100) Single Crystal

L. P. WANG, C. SOTO, AND W. T. TYSOE[1]

Department of Chemistry and Laboratory for Surface Studies, University of Wisconsin, Milwaukee, Wisconsin 53211

Received March 22, 1993; revised April 29, 1993

It is shown, using a high-pressure reactor incorporated into an ultrahigh-vacuum chamber, that an initially clean molybdenum (100) single crystal can catalyze propylene metathesis. The reaction is found to be first-order in propylene pressure which proceeds with a high activation energy (~65 kcal/mol). Auger spectroscopy reveals the presence of a thick (~10 monolayers) carbonaceous layer on the surface of the catalyst following reaction. It is further demonstrated, using restart reactions, that metathesis proceeds in presence of this layer. However, the reaction prefactor is $\sim 8 \times 10^{12}$ site^{-1} s^{-1} so that the reaction appears not to be drastically inhibited by the presence of the carbonaceous layer, rather, the high reaction activation energy is primarily responsible for the low rate. Methylcyclopropane and hydrogenolysis products are also formed in the reaction, an observation that is consistent with the reaction proceeding at the surface via the "carbene" mechanism.

INTRODUCTION

Molybdenum-based materials catalyze a wide range of hydrocarbon and heteroatom-containing hydrocarbon conversion reactions. These include heteroatom removal reactions such as hydrodesulfurization (*1*, *2*), as well as alkene hydrogenation (*3–8*), hydrogenolysis (*9*, *10*), carbon monoxide hydrogenation (*11*), and olefin metathesis (*12*, *13*). In many of these catalysts, the molybdenum is, however, often chemically modified so that molybdenum *disulfide* is used to catalyze hydrodesulfurization (*1*, *2*) and olefin metathesis is catalyzed by a molybdenum oxide (*12*, *15*), and while Group VI metals do catalyze hydrogenation, the carbide is invariably found to be more effective, exhibiting hydrogenation activities more akin to those observed over the noble metals (*3–8*). The following focusses in particular on olefin metathesis catalyzed by a metallic molybdenum single crystal using an isolatable high pressure reactor incorporated into an ultrahigh-vacuum (UHV) chamber.

Metallic molybdenum is not conventionally thought of as being active for the catalysis of olefin metathesis (*16*, *17*). However, investigations of the activity of various oxides of molybdenum supported on molybdenum foil show that MoO_2 provides an effective catalyst but that both molybdenum metal and MoO_3 do catalyze the reaction, but with an activity significantly less than for MoO_2 (*18*). The advantage of studying this reaction on a structurally well-characterized Mo(100) single crystal surface is that they can be easily prepared and compared with the results of the chemistry of the reactants on these surfaces.

Olefin metathesis was first discovered by Banks and Bailey (*19*), and subsequently a wide range of both homogeneous and heterogeneous metathesis catalysts were discovered. The majority of mechanistic investigations into olefin metathesis have focussed on *homogeneously* catalyzed reactions (*20–24*). In this case, the currently most widely accepted model holds that the

[1] To whom correspondence should be addressed.

0021-9517/93 $5.00

initial step in metathesis is carbon–carbon bond cleavage to form carbene ligands which provide the catalytically active sites. Further alkene reacts with this carbene forming a metallocycle which subsequently decomposes by the reverse of this reaction to form metathesis products. The catalytic activity is therefore proposed to derive from the initial decomposition of the alkene to form active carbenes. There is, in addition, strong evidence that this mechanism also applies in heterogeneous phase (*25*, *26*). UHV experiments on Mo(100) show that adsorbed ethylene rapidly dissociates into adsorbed CH_x species on this surface, suggesting that the initial carbene formation step on metallic molybdenum is facile (*27*). The kinetics of the reaction are therefore examined in the following to probe the origin of such low activity in spite of the apparent ease of carbon–carbon bond cleavage in adsorbed alkenes on Mo(100).

2. METHODS

The apparatus used for the catalytic experiments has been described in detail in previous publications (*28*, *29*). The salient feature of the apparatus for the purposes of the results presented here is the incorporation in the UHV chamber of an isolatable high-pressure reactor. The UHV chamber itself is a bakeable, stainless-steel chamber that operates at a base pressure of 1×10^{-10} Torr (1 Torr = 133.3 N m^{-2}) following bakeout. It is equipped with an RFA for Auger and LEED measurements and a quadrupole mass spectrometer for leak testing, residual gas analysis and thermal desorption spectroscopy. The sample is mounted to the end of a rotatable, coaxial sample manipulator, and the sample temperature can be varied between 80 and 2000 K. It can also be enclosed in a small volume reactor and isolated from UHV. The cell is sealed by an annealed copper gasket and, once sealed, the pressure in the UHV portion of the apparatus can be maintained at $<5 \times 10^{-10}$ Torr with the cell pressurized to 1 atm. The reaction cell is connected to an external loop equipped with a recirculation pump, capacitance manometer, and sampling valve for diverting a portion of the reaction mixture to a gas chromatograph for analysis. The cell therefore operates as a recirculating batch reactor and reaction rates are measured directly from the product accumulation curve for low ($\ll 1\%$) conversions. It is found for all the reactions described below that the product accumulation curves are linear over this conversion range. It has already been demonstrated that this apparatus reproduces the kinetics for ethylene hydrogenation catalyzed by Mo(100) extremely well (*28*). The absolute reaction rates can be determined from the gas chromatograph trace by scaling the product concentrations to the signal of the reactant propylene assuming that the sensitivity of the flame-ionization detector is proportional to the number of carbons in the hydrocarbon. Reaction products are identified from their retention times, which were calibrated by filling the reaction loop with known mixtures of gases and measuring the retention times under exactly identical conditions as used for product analysis during reaction. The column used for these reactions was a 100-cm length of Poropak which was capable of separating ethylene from acetylene. Finally, the nature of the reaction products was also verified by leaking a portion of the gas mixture from the cell into the UHV chamber via a variable leak valve following a reaction. In this way, an additional mass spectroscopic analysis of the reaction products could be obtained using the quadrupole mass analyzer and compared with the fragmentation patterns of known compounds.

The sample was cleaned using a standard procedure and was adjudged clean when no signals due to adsorbed contaminants (e.g., carbon or oxygen) were detected in Auger spectroscopy. In addition, no oxygen was detected on the surface of the sample using Auger spectroscopy following reaction. However, since surface oxygen could be obscured by the carbon present on the surface

following reaction (see below), thermal desorption spectroscopy provides a significantly more stringent test for the presence of any surface oxygen. The complete absence of oxygen on the surface was further verified since no carbon monoxide or carbon dioxide was detected from the sample following reaction using temperature-programmed desorption.

The reactant (propylene; Union Carbide, Linde; 99.9%) was purified by several bulb-to-bulb distillations using an all-glass gas handling line and keeping only the middle portion of the distillate. The gas was stored in glass until use. The purity of the resulting propylene was checked mass-spectroscopically and using gas chromatography.

3. RESULTS

The detection of C_4 compounds, consisting of 2-butene, and also ethylene following reaction over a Mo(100) single crystal confirms that olefin metathesis is catalyzed by initially clean *metallic* molybdenum according to the reaction

$$2C_3H_6 \rightarrow C_2H_4 + C_4H_8.$$

The stoichiometry of this equation indicates that C_2 and C_4 hydrocarbons are formed in this reaction in equimolar amounts. Figure 1 shows the accumulation curves for olefin metathesis products formed by the reaction of propylene catalyzed by a Mo(100) single crystal sample using a propylene partial pressure of 70 Torr at sample temperatures between 818 and 880 K. Note that the total cell pressure in all reactions was maintained at 800 Torr using nitrogen to ensure that an adequate and identical gas recirculation rate was used in all experiments. Shown in Fig. 2 is a histogram comparing the rates for the same reaction over molybdenum and also catalyzed by both iron and palladium foils using otherwise identical experimental conditions. These results show that iron can also catalyze olefin metathesis but at a lower rate than when molybdenum is used. Palladium shows essentially no activity and no reaction products were observed in this case. Note that, in these experiments, exactly identical sample mounting schemes were used and only the sample was changed. These results then also confirm that the reaction is indeed catalyzed by the Mo(100) single crystal sample and that products are

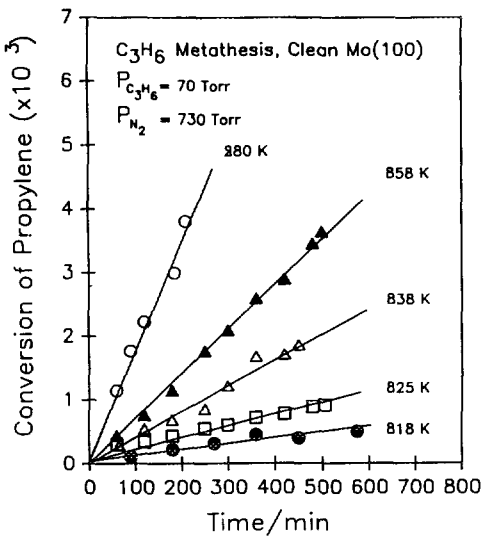

FIG. 1. Plots of the product accumulation curves for propylene metathesis catalyzed by a Mo(100) single crystal obtained as a function of reaction temperature between 818 and 880 K, using a partial pressure of 70 Torr of propylene. Reaction temperatures are indicated adjacent to the corresponding curve.

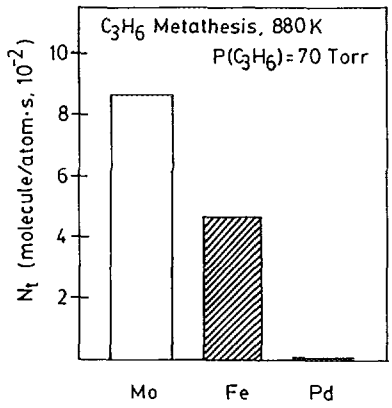

FIG. 2. A histogram showing relative rates of propylene metathesis catalyzed by molybdenum, iron and palladium for reaction at 880 K using a propylene partial pressure of 70 Torr.

not due to experimental artifacts or gas-phase reactions.

Kinetics of Propylene Metathesis

Shown in Fig. 1 are product accumulation curves for propylene metathesis obtained as a function of catalyst temperature using an alkene partial pressure of 70 Torr. Conversions are, in all cases, less than 1% and reaction rates are measured from the slopes of the product accumulation curves. Shown in Fig. 3 is the corresponding Arrhenius plot of ln (N_t), where N_t is the turnover frequency, versus $1/T$. Turnover frequencies N_t are calculated by normalizing the reaction rate to the area of a square surface unit cell on the (100) face of clean molybdenum (which has an area of 1×10^{-15} cm^2) (*26*). This assumption takes no account of site blockage by carbonaceous deposits (see below) and so implies that the calculated value is a lower bound for the turnover frequency. An activation energy of 65 ± 5 kcal/mol is measured for this reaction from the slope of the curve. The value of the activation energy for metathesis catalyzed by Mo(100) measured here is considerably higher than that generally observed on supported oxide catalysts (*30*, *31*). The activation energy for active catalysts derived from $Mo(CO)_6$ on alumina is ~7.3 kcal/mol (*32*, *33*) and that for supported molybdenum oxide ranges between 8.0 and 9.0 kcal/mol (*34*, *35*). This, however, is in line with the observation that molybdenum in a zero oxidation state is *not* a vigorous catalyst for olefin metathesis.

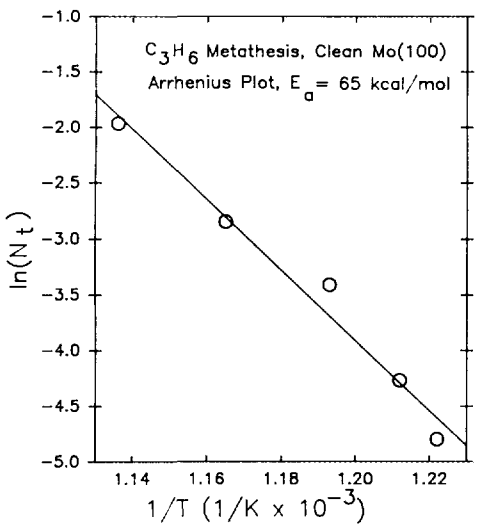

FIG. 3. Kinetic data for Mo(100)-catalyzed propylene metathesis displaying the temperature dependence plotted in Arrhenius form. Measurement of the slope yields a reaction activation energy of 65 ± 5 kcal/mol.

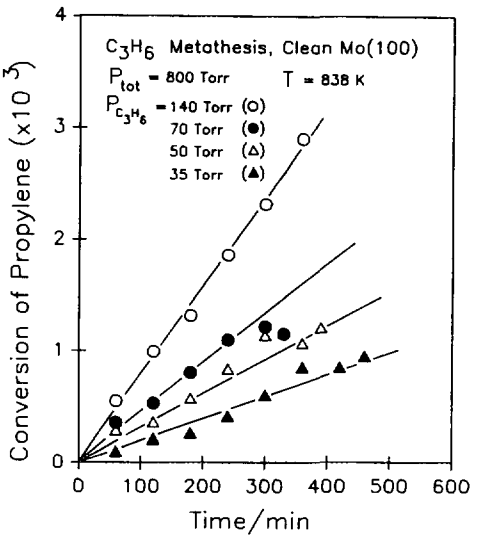

FIG. 4. Plots of the product accumulation curves for propylene metathesis catalyzed by a Mo(100) single crystal obtained as a function of pressure in the range 35 to 140 Torr using a reaction temperature of 838 K.

Product accumulation curves are also shown in Fig. 4, in this case obtained as a function propylene partial pressure, for a reaction temperature of 838 K. The total cell pressure in these experiments is again maintained at 800 Torr using nitrogen. The results show that the reaction rate increases with propylene partial pressure. The resulting pressure dependencies are summarized on Fig. 5, which plots the log of the reaction rate (ln (rate)) versus the log of the reactant partial pressures (ln (pressure)). Measurement of the slope of this curve indicates that the reaction order is 1.0 ± 0.1 for Mo(100)-catalyzed propylene metathesis in the pressure range 35 to 140 Torr. The ki-

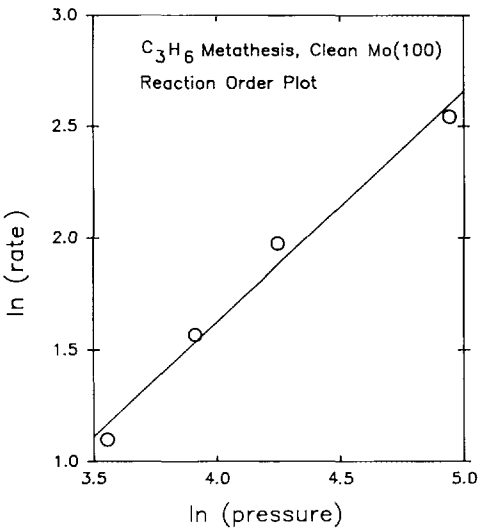

FIG. 5. Kinetic data for Mo(100)-catalyzed olefin metathesis displaying the pressure dependence plotted as ln (rate) versus ln (pressure). The slope yields a reaction order of 1.0 ± 0.1.

netic data for propylene metathesis catalyzed by initially clean Mo(100) can be summarized as

$$r_m = 8 \pm 2 \times 10^{12} p(C_3H_6)^{1.0\pm0.1} \exp(-65 \pm 5 \times 10^3/RT)/\text{site/s}, \quad (1)$$

where r_m is the rate of propylene metathesis measured as a turnover frequency (i.e., reactions/site/s, where the rates are normalized to the square unit cell on the Mo(100) surface), $p(C_3H_6)$ is the propylene partial pressure (measured in Torr), and T the absolute temperature. The reaction preexponential factor ($8 \pm 2 \times 10^{12}$ site^{-1} s^{-1} Torr^{-1}) is calculated from the intercept of the Arrhenius plot (Fig. 3) using the first-order pressure dependence measured in Fig. 5.

In addition to the metathesis reaction, other products were also noted which could be ascribed to hydrogenolysis products (i.e., the formation of methane and ethylene) and also the formation of small, but detectable, amounts of methylcylopropane. Note that throughout the reaction the number of moles of ethylene were equal to the sum of the number of moles of methane and butene and so maintained a carbon mass balance.

Nature of the Surface during Reaction

The surface of the Mo(100) single crystal was analyzed following reaction using Auger spectroscopy and in all cases large carbon signals were measured. The resulting amount of surface carbon is indicated in Fig. 6 measured from the peak-to-peak amplitude of the carbon Auger peak (at 271 eV kinetic energy) normalized that of the substrate peak (measured also from the peak-to-peak amplitude of the molybdenum Auger transition at 221 eV kinetic energy), designated $I(C)/I(Mo)$, which is plotted as a function of the reaction temperature (●). The reactant pressure in all cases was 70 Torr. The Auger ratio has been approximately related to the film thickness (*28*) using a standard value for the electron mean free path and a calibration for the Auger sensitivities for a surface covered with half

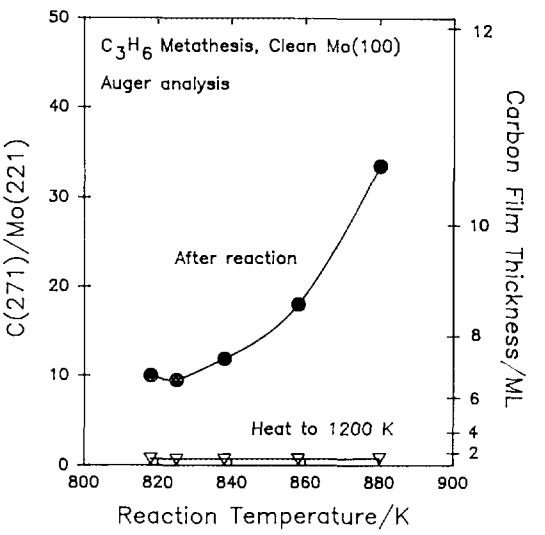

FIG. 6. The amount of accumulated carbon detected on the Mo(100) surface plotted as a function of reaction temperature (●) following reaction with propylene (70 Torr) using the high-pressure reactor and measured from the C(271)/Mo(221) Auger ratio. Plotted also the abscissa are the film thicknesses calculated as outlined in the text. Shown also are the Auger ratios (▽) measured after annealing each of the surfaces to 1200 K.

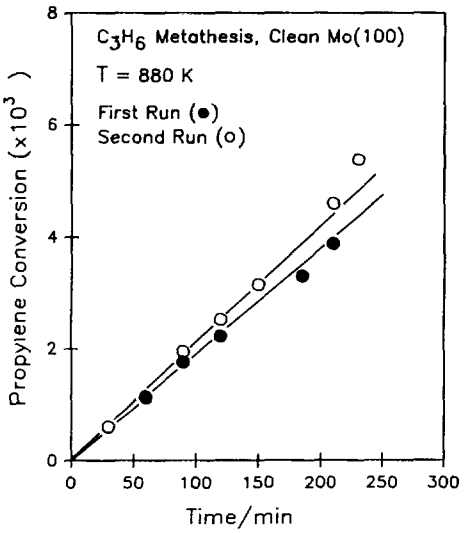

FIG. 7. Product accumulation curve obtained following reaction of propylene (70 Torr) over a Mo(100) single crystal at 880 K (●). The sample was then removed from the cell into UHV, the surface analyzed using Auger spectroscopy, and the reaction restarted using identical reaction conditions. The resulting product accumulation curve is also shown (○).

a monolayer of carbon. This yields a formula relating the film thickness t to the Auger intensity ratio $I(C)/I(Mo) = r$ as

$$r = C(\exp(t/\lambda) - 1), \qquad (2)$$

where $C = 1.63$ and $\lambda = 3.5$. The resulting *approximate* values of film thickness derived using this method are also plotted onto the data of Fig. 6 indicating that a maximum of approximately the equivalent of ten to eleven layers of carbon are present on the surface. The film thickness clearly increases significantly as the reaction temperature increases. A similar large surface carbon Auger signal was noted following Mo(100)-catalyzed ethylene hydrogenation (*28*).

Note that the total number of turnovers during a reaction exceeds 2000, indicating that the metathesis reaction proceeds in the presence of this carbonaceous layer. This point in emphasized by the data of Fig. 7, which show the results of a "restart" reaction. In this case, a metathesis reaction is run on an initially clean Mo(100) sample and the resulting product accumulation curve is shown in Fig. 7 as filled circles (and corresponds to the completion of ~2000 reactions per site, assuming one site per surface unit cell on Mo(100)). The sample was then removed from the reaction cell into UHV and the carbon coverage measured using Auger spectroscopy, which confirmed the presence of approximately the equivalent of ten monolayers of carbon on the surface. The sample was then reinserted into the cell and the reaction continued using exactly identical conditions, i.e., 70 Torr of propylene at a reaction temperature of 880 K. The resulting product accumulation curve for the second run is shown in Fig. 7 as open circles and indicates that the reaction rate is essentially identical and, moreover, continues for a further 2000 turnovers confirming that the metathesis reaction indeed proceeds in the presence of a significant thickness of carbon on the surface.

The thermal stability of this carbonaceous layer was investigated by measuring the C(271)/Mo(221) Auger ratio after annealing the carbon-covered surface to various temperatures following reaction at 818, 838, and 858 K. The results are displayed in Fig. 8, which plots the ratio of the carbon Auger signal to the molybdenum Auger signal (which is designated C(271)/Mo(221)) as a function of annealing temperature. In addition, axes showing approximate film thicknesses, calculated using Eq. (2), are also indicated. For all surfaces, the film thickness remains reasonably constant up to an annealing temperature of ~900 K, and then exhibits a precipitous decrease, so that after heating the surface to 1100 K, the carbon coverage has significantly decreased and remains constant thereafter. The final C(271)/Mo(221) Auger ratio measured after annealing to 1300 K is also plotted on Fig. 6 for surfaces formed after reaction at various temperatures (▽). In each case, the carbon/molybdenum Auger ratio is identical at 0.5 ± 0.1, which corresponds to a surface

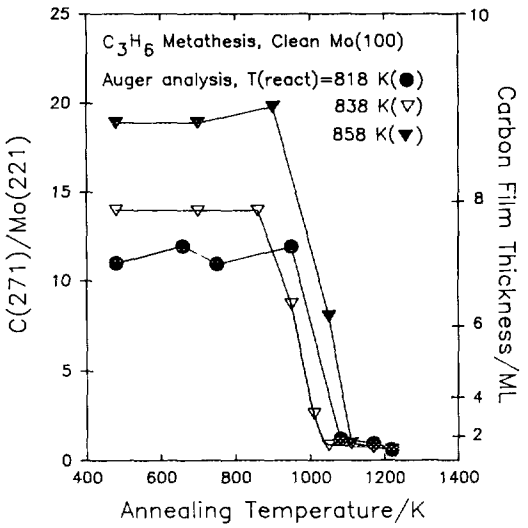

FIG. 8. Plot of the C(271)/Mo(221) Auger ratio for the Mo(100) single crystal covered with carbonaceous deposit as a function of annealing temperature after reaction in propylene: (●) after reaction at 818 K, (▽) after reaction at 838 K, and (▼) after reaction at 858 K.

carbon coverage, $\Theta(C) = 1.0 \pm 0.2$ (where the carbon coverage is in this case referred to the number of unit cells on Mo(100)).

The thermal desorption spectra obtained for the carbon-covered surface after reaction are shown in Fig. 9 (taken using a heating rate of ~30 K/s). Since the mass spectrometer used for these experiments is capable of monitoring only a single mass, each of these spectra were obtained after different reactions. The spectra of Fig. 9 show significant H_2 (2 amu) desorption, which implies the presence of large amount of hydrogen on the surface indicating that hydrogen is available for the formation of hydrogenolysis products described above. In addition, mass spectrometer signals are detected during thermal desorption at 16, 14, and 12 amu in the temperature range corresponding to that over which a significant depletion of surface carbon is measured by Auger spectroscopy (Fig. 8; 900–1100 K). The observed decrease in carbon coverage is ascribed to hydrocarbon desorption.

4. DISCUSSION

The results of Figs. 1 and 4 indicate that olefin metathesis is catalyzed by initially clean, metallic molybdenum. Care was taken to completely exclude oxygen from the reaction and the complete absence of oxygen on the surface was confirmed following reaction using both Auger spectroscopy and thermal desorption spectroscopy. The activation energy for the reaction measured from the Arrhenius plot shown in Fig. 3 is 65 ± 5 kcal/mol and the reaction is first order (1.0 ± 0.1) in propylene pressure between 35 and 140 Torr (Fig. 5). The resulting measured reaction kinetics are displayed in Eq. (1). The results of Fig. 2 confirm that the reaction is catalyzed by the initially clean Mo(100) single crystal and not, for example, by the sample supports since a palladium sample shows no activity for olefin metathesis. An iron sample does show some activity (Fig. 2), and this is discussed in greater detail below.

The *homogeneously* catalyzed olefin me-

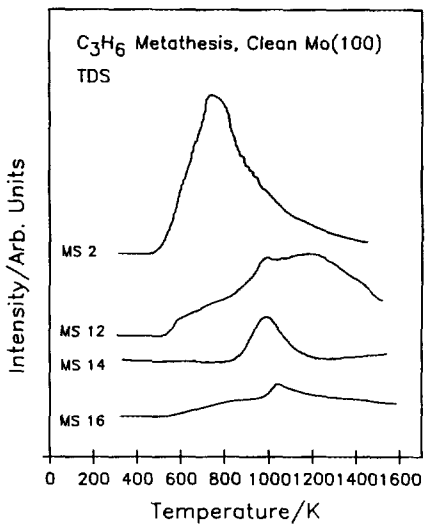

FIG. 9. Plots of the thermal desorption spectra obtained following reaction of the Mo(100) single crystal in propylene taken at 2, 12, 14, and 16 amu. The heating rate used for these experiments was 30 K/s. Note that each of these spectra were collected following different reactions.

tathesis reaction has been proposed to proceed by an initial formation of a surface carbene which provides the catalytically active site (*20–26*). Subsequent reaction is suggested to occur at this active site by the formation of a metallocycle which decomposes by the reverse of its formation reaction yielding metathesis products. There is strong evidence that a similar mechanism operates on supported metathesis catalysts (*25*, *26*). The products detected from the reaction of propylene is consistent with this reaction scheme. For example, the detection of hydrogenolysis products (methane and ethylene) from the reaction of propylene with low oxidation state, supported molybdenum has been observed previously (*9*, *10*) and indicates that the molybdenum surface is capable of dissociating propylene into C_1 and C_2 moieties. In addition, the detection of a cyclic products is consistent with the presence of an intermediate metallocycle on the surface, and such cyclization reactions have also been observed on low-oxidation-state catalysts (*36*).

Surface chemistry experiments on the adsorption of both ethylene (*27*) and propylene (*37*) on Mo(100) carried out in UHV indicate that the carbon–carbon double bonds in the alkene cleave following initial adsorption at 80 K and after warming to room temperature. This implies that double bond cleavage is an efficient process on metallic molybdenum since it occurs even under ultrahigh-vacuum conditions and suggests that carbene formation on molybdenum should be extremely facile. A similar cleavage of the ethylenic double bond to form carbene has also been observed on iron using photoelectron spectroscopy (*38*, *39*). The observation of metathesis products from the reaction of propylene using an iron catalyst is consistent with this surface chemistry and the operation of the carbene mechanism in the surface reaction. It is also consistent with the measurement of a relatively large preexponential factor suggesting a large "active site" density on Mo(100).

The overall rate of olefin metathesis catalyzed by metallic molybdenum measured in these experiments is small in comparison with conventional oxide catalysts. The rapid formation of the carbene, which is observed to occur even in UHV, would seem to suggest that the carbene "active site" concentration on the Mo(100) catalyst should be very large and that this should lead to a correspondingly high metathesis rate. We therefore now turn our attention to examining possible origins of this lower catalytic reaction rate when metallic molybdenum is used as a catalyst. Two possible culprits can be identified. First is the presence of the thick carbonaceous layer observed on the surface of the Mo(100) model catalyst during reaction (Figs. 6 and 7). The second possible reason for the low activity is large activation energy for the reaction.

Role of the Surface Carbonaceous Layer

The presence of a significant amount of surface carbon is detected during the olefin metathesis reaction, and the amount of carbon at the surface increases with reaction temperature (Fig. 6). Note that the presence of a carbonaceous layer appears to be a common feature in hydrocarbon reactions over supported molybdenum-derived catalysts (*40–45*). Since this carbonaceous layer thickness is constant even after ~2000 turnovers, it is likely to be present on the surface with an equilibrium thickness during essentially the entire course of the reaction. That is, the reaction proceeds in the presence of this carbonaceous layer. This notion is confirmed by the results presented in Fig. 7, which show that the metathesis rate is identical following a "restart" reaction, so that the reaction proceeds at the same rate on a surface that is covered with a carbonaceous layer as on the initially clean sample.

The thermal stability of this layer is displayed in Fig. 8, which shows that the layer thermally decomposes at ~1000 K finally depositing a monolayer of carbon. This decomposition temperature is essentially identical to the decomposition temperature of the layer formed during Mo(100)-catalyzed

ethylene hydrogenation (*28*) suggesting that the layers are chemically identical in both cases. It was suggested, in the case of ethylene hydrogenation (*28*), that the reactants (ethylene and hydrogen) had to permeate this carbonaceous layer to gain access to the surface and that this contributed to the low activity of molybdenum as a hydrogenation catalyst compared top the noble metals. Note, however, that the reaction pre-factor measured experimentally for olefin metathesis ($8 \pm 2 \times 10^{12}$ site^{-1} s^{-1} Torr^{-1}) is large, suggesting that the reactants, in fact, *are* able to penetrate this layer. These results suggest, therefore, that the primary reason for the low olefin metathesis rate when catalyzed by Mo(100) must be the very high value of activation energy for the reaction catalyzed by initially clean Mo(100) which is 65 ± 5 kcal/mol compared to typical values for active metathesis catalysts (~7–9 kcal/mol (*32–35*)). This is not to imply that the presence of the relatively thick carbonaceous layer has no effect on the overall activity since its presence must, to some extent, inhibit access of the reactant to the catalyst surface.

In the case of ethylene hydrogenation (*28*), apart from the low reaction rate, the pressure dependencies and activation energies were very typical of transition-metal-catalyzed hydrogenation reactions suggesting that the surface reaction was similar to that on, for example, noble metals. The results for Mo(100)-catalyzed metathesis (this work) suggest that the hydrocarbons can indeed penetrate the carbonaceous layer, so that the low prefactor in that case (3×10^3 compared to 7×10^6 for platinum-catalyzed hydrogenation (*46*)) must also be ascribed to blocking of reaction sites, presumably by the surface carbonaceous layer.

5. CONCLUSIONS

Metallic molybdenum catalyzes propylene metathesis forming both ethylene and butene, but with a rather low reaction rate and high activation energy. The activation energy for the reaction catalyzed by Mo(100) is significantly higher than commonly observed for supported molybdenum oxide metathesis catalysts (7–9 kcal/mol (*32–35*)). Surface science experiments show that alkenes can dissociatively adsorb on the Mo(100) surface, in line with proposed "carbene" mechanisms for olefin metathesis. In addition, the detection of methyl cyclopropane and hydrogenolysis products is consistent with this reaction route. The large activation energy observed for the Mo(100)-catalyzed reaction (~65 kcal/mol) in conjunction with the observed facile carbon–carbon double bond cleavage suggests that metallocycle formation or decomposition is the rate-limiting step in the reaction. A thick carbonaceous layer is also found to form on the Mo(100) surface during propylene decomposition. Restart reactions suggest that olefin metathesis takes place in the presence of this carbonaceous layer and that the resultant thickness of the film is the result of an equilibrium between propylene decomposition at the metal surface, and its thermal decomposition. It is suggested that the presence of the carbonaceous deposit does not primarily limit the rate of metathesis since a relatively large value of prefactor is measured for this reaction and that the low rate is due to the large activation energy.

ACKNOWLEDGMENTS

We gratefully acknowledge support of this research by the Department of Energy, Division of Chemical Sciences, Office of Basic Energy Sciences (Grant FG02-92ER14298) and the University of Wisconsin Graduate School. We are also grateful to J. Jacobs for assistance in the design and modification of the isolatable high-pressure reactor.

REFERENCES

1. Gellman, A. J., Farias, M. H., and Somorjai, G. A., *J. Catal.* **88,** 564 (1984).
2. Gellman, A. J., Farias, M. H., and Somorjai, G. A., *Surf. Sci.* **136,** 217 (1984).
3. Sinfelt, J. H., and Yates, D. J. C., *Nature Phys. Sci.* **229,** 27 (1971).
4. Boudart, M., Oyama, S. T., and Leclerq, L., in "Proceedings, 7th International Congress on Catalysis, Tokyo, 1980" (T. Seiyama and K. Tanabe, Eds.), p. 578. Elsevier, Amsterdam, 1981.
5. Leary, K. J., Michaels, J. N., and Stacey, A. M., *J. Catal.* **101,** 301 (1986).

6. Bowman, R. G., and Burwell, R. L., Jr., *J. Catal.* **63,** 463 (1980).
7. Bowman, R. G., and Burwell, R. L., Jr., *J. Catal.* **88,** 388 (1984).
8. Kouskova, A., Adamek, J., and Ponec, V., *Collect. Czech. Chem. Commun.* **35,** 2538 (1970).
9. Nakamura, R., Pioch, D., Bowman, R. G., and Burwell, R. L., Jr., *J. Catal.* **93,** 388 (1985).
10. Nakamura, R., Bowman, R. G., and Burwell, R. L., Jr., *J. Am. Chem. Soc.* **103,** 673 (1981).
11. Logan, M., Gellman, A. J., and Somorjai, G. A., *J. Catal.* **63,** 226 (1980).
12. Mol, J. C., and Moulijn, J. A., *Adv. Catal.* **24,** 131 (1975).
13. Rooney, J. J., and Stewart, A., *Catalysis* **1,** 277 (1977).
14. Grubbs, R. H., *Prog. Inorg. Chem.* **24,** 1 (1978).
15. Höcker, J., Reimann, W., Reif, L., and Riebel, K., *J. Mol. Catal.* 191 (1980).
16. Brenner, A., And Burwell, Jr., R. L., *J. Catal.* **52,** 364 (1978).
17. Burwell, R. L., Jr., and Brenner, A. J., *J. Mol. Catal.* **1,** 77 (1975).
18. Bartlett, B., Soto, C., Wu, R., and Tysoe, W. T., *Catal. Lett.*, in press.
19. Banks, R. L., and Bailey, G. C., *Ind. Eng. Chem. Prod. Res. Dev.* **94,** 60 (1965).
20. Cardin, D. J., Doyle, M. J., and Lappert, M. F., *J. Chem. Soc. Chem. Commun.*, 927 (1972).
21. Fischer, E. O., and Dorner, B., *Chem. Ber.* **107,** 1156 (1974).
22. Greenlee, W. S., and Farona, M., *Inorg. Chem.* **15,** 2129 (1976).
23. Katz, T. J., and McGinnis, J., *J. Am. Chem. Soc.* **97,** 1592 (1975).
24. Grubbs, R. H., and Hoppin, C. R., *J. Am. Chem. Soc.* **1010,** 1499 (1979).
25. Kazuta, M., and Tanaka, K., *Catal. Lett.* **1,** 7 (1988).
26. Vikulov, K. A., Elev, I. V., Shelomov, B. N., and Kazamsky, V. B., *Catal. Lett.* **2,** 121 (1989).
27. Wang, L. P., and Tysoe, W. T., *Surf. Sci.* **230,** 74 (1990).
28. Wang, L. P., and Tysoe, W. T., *J. Catal.* **128,** 320 (1991).
29. Wang, L. P., Millman, W. M., and Tysoe, W. T., *Catal. Lett.* **1,** 159 (1988).
30. Bradshaw, C. P., Hownan, E. J., and Turner, L., *J. Catal.* **7,** 269 (1967).
31. Ogata, E., and Kamiya, Y., *Ind. Eng. Chem. Prod. Res. Dev.* **13,** 226 (1974).
32. Davie, E. S., Whan, D. A., and Kemball, C., *J. Catal.* **24,** 272 (1972).
33. Howe, R. F., Davidson, D. E., and Whan, D. A., *J. Chem. Soc. Faraday Trans. 1* **68,** 2266 (1972).
34. Moffat, A. J., and Clark, A., *J. Catal.* **17,** 264 (1970).
35. Luckner, R. C. McConocie, G. E., and Wills, G. B., *J. Catal.* **28,** 63 (1973).
36. O'Neill, P. P., and Rooney, J. J., *J. Am. Chem. Soc.* **94,** 4383 (1972).
37. Wang, L. P., and Tysoe, W. T., *Surf. Sci.* **245,** 41 (1991).
38. Brucker, C., and Rhodin, T., *J. Catal.* **47,** 214 (1977).
39. Rhodin, T., Brucker, C. F., and Anderson, A. B., *J. Chem. Phys.* **82,** 354 (1978).
40. Briggs, D., Dewing, J. Barden, A. G., Moyes, R., and Wells, P. B., *J. Catal.* **65,** 31 (1980).
41. Páal, Z., Thomson, S. J., Webb, G., and McCorkindale, N. J., *Acta. Chim. Hung.* **84,** 445 (1975).
42. Nakamura, J., Tanaka, K.-I., and Toyoshima, I., *J. Catal.* **108,** 55 (1987).
43. Hattori, T., and Burwell, R. L., Jr., *J. Phys. Chem.* **83,** 241 (1979).
44. Gupta, N. M., Kamble, V. S. and Iyer, R. M., *J. Catal.* **88,** 457 (1984).
45. Amariglio, A., and Amariglio, H., *J. Catal.* **78,** 44 (1982).
46. Zaera, F., and Somorjai, G. A., *J. Am. Chem. Soc.* **106,** 2288 (1984).